

## Extraction and Analysis of Coronary-tree from single X-ray Angiographies

erschien in

```
@inproceedings{Koehler2004EAA,  
crossref = {proceedings2004POS},  
author = {Koehler, Hildegard and Couprie, M. and Bouattour, Sahla and Paulus, Dietrich},  
title = {Extraction and Analysis of Coronary-tree from single X-ray Angiographies},  
note = {to appear}  
}
```

```
@proceedings{proceedings2004POS,  
year = {2004},  
title = {proc. of SPIE International Symposium Medical Imaging},  
booktitle = {proc. of SPIE International Symposium Medical Imaging}  
}
```

# Extraction and Analysis of Coronary-tree from single X-ray Angiographies

Hildegard Koehler<sup>a</sup>, Michel Couprie<sup>b</sup>, Sahla Bouattour<sup>a</sup> and Dietrich Paulus<sup>a</sup>

<sup>a</sup> University of Koblenz-Landau, Universitaetsstrasse 1- 56070 Koblenz, Germany;

<sup>b</sup> Laboratoire Algorithmique et Architecture des Systèmes Informatiques, ESIEE, 2 Bd Blaise Pascal - B.P. 99 93162 Noisy-Le-Grand CEDEX, France

## ABSTRACT

Coronary vessel abnormalities can lead to insufficient blood circulation in the heart muscle. One way to control and detect distributions of this supply is the continuous observation of the vessel structure of the patient over a certain time. In this paper we propose a reliable method for extracting the main vessels and most notably also fine ramifications in noisy angiographies with uneven background. We structured the extracted centerlines in a graph, obtaining thus information about the depth of branching-out and the number of visible vessels in the coronary-tree. These quantitative measurements serve as indicators to categorize the state of recovery of the patient and can be compared to earlier or later disease-stages. We evaluated our methods by comparing the results with hand-segmented images.

**Keywords:** coronary-tree segmentation, midline extraction, bifurcation detection, graph based coronary-tree modeling, segmentation evaluation

## 1. INTRODUCTION

Diagnosis and therapy of coronary stenosis is a usual praxis in cardiology. Usually examinations are made by an angiography to localize the abnormality. The stenosis can be treated or removed by an *angioplasty*. The stenosis has mostly a direct influence on blood circulation and the nutrition of especially finer ramifications. Even after successful treatment, the physician should control the insufficiency of finer vessels to guarantee normal functioning of all vessels. Physicians are used to compare *by-hand* the X-ray images taken before and after the treatment. The development of an automatic method to evaluate these images would help the physician to make the diagnosis and would improve the workflow of treatment.

The segmentation of coronary vessels, and precisely the extraction of centerlines is addressed by many researchers within different contexts other than heart segmentation such as retina vessel segmentation or road segmentation.<sup>1,2</sup> State of the art methods differ in assuming an explicit or an implicate model for the vessel structure. Most of them perform a scale-space analysis<sup>3</sup> to extract vessels of all diameters. The recognition of bifurcations and detection of crossings represent one of the main problems. The usage of Digital subtraction angiography (DSA)<sup>4</sup> to enhance the coronary-tree from the uneven, noisy background of angiographic images is not possible due to body motion during acquisition.

In this contribution we present a reliable method to extract main arteries as well as finer vessels and ramifications from angiographies with uneven and irregular illuminated background. The structure of the extracted vessels will be stored in a graph, containing also local information on width, orientation and brightness of the vessels. These informations can be compared with earlier and later disease states to judge the effectiveness of a treatment on patients. Furthermore we propose a method for evaluating segmentation result.

In section 2 we present the method used to extract the vessels from background. Section 3 describes the centerline extraction, graph modelling, as well as bifurcation and crossings detection. Section 4 presents the results of the approach, examines the correctness and completeness of segmentation and analysis and discusses the related problems. Finally section 5 concludes the present work and gives an overview on future work.

---

E-mail: koehlerh@uni-koblenz.de

E-mail: bouattour@uni-koblenz.de

## 2. EXTRACTION OF CORONARY-TREE

A reliable segmentation of vessels of all diameters is a crucial step in the proposed procedure, because it has a direct impact on the centerline extraction, as well as the recognition of bifurcations and the labeling of the branching-graph. The general requirement to segmentation is in this context also valid: it should enhance the present structure, eliminates noise while preserving even fine details of the anatomy.

The application of the digital subtraction angiography technique (DSA) to remove the background out of the X-ray angiographies cannot be applied due to the physiological conditions of the acquisition such as respiration and cardiac motion. The developed approach has thus to deal with noisy, uneven background and to be able to extract also fine vessels. In addition to that ambiguities caused by vessel crossings, overlaps and loops have to be resolved. The current tendency in the processing of angiographies is to use *artificial* DSA approaches, which are basically based on morphological operators to extract the background.<sup>5</sup> In the following sections we propose a combined approach based on the separation of clearly visible vessels from the surrounding background using morphological technique, followed by an extraction of fine vessels by applying a modified Gabor filter. The combination of these techniques would lead to robust extraction of the coronary-tree, without requiring DSA, or user intervention.

### 2.1. Linear Tophat-Operator (LTO)

The basic idea of artificial DSA using morphological filter is to find an operator which filters out just the interesting structures (here vessels) and keeps the background as intact as possible. The gained background image is then subtracted from the original to get the vessels.

The Tophat operator is a morphological opening operator,<sup>6</sup> which performs an erosion  $\epsilon_B(f)$  followed by a dilation  $\delta_B(f)$ , where  $B$  denotes the structure element (SE) and  $f$  is the set of image points. The Tophat operator is given by

$$TH_\gamma(f) = f - \gamma(f)$$

where  $\gamma(f) = \delta_{\bar{B}}(\epsilon_B(f))$  stands for the opening operation. The choice of the structural element is the main problem in this approach, because it should be complementary to the interesting structure. In fact by filtering the image by a certain SE, all elements which do not have the form of SE will be eliminated. Vessels exhibit several properties that should be taken into consideration: they have *curved*, *tubed* form with different diameters. Furthermore, vessel similar structure such as rips should be preserved as a part of the background. A fortiori we choose a line segment to model the transversal section of vessels. Its length should correspond at least to the maximal diameter of vessels and its direction will vary to retrieve vessels in all directions. Figure 1 illustrates the opening result by a line segment in one direction.

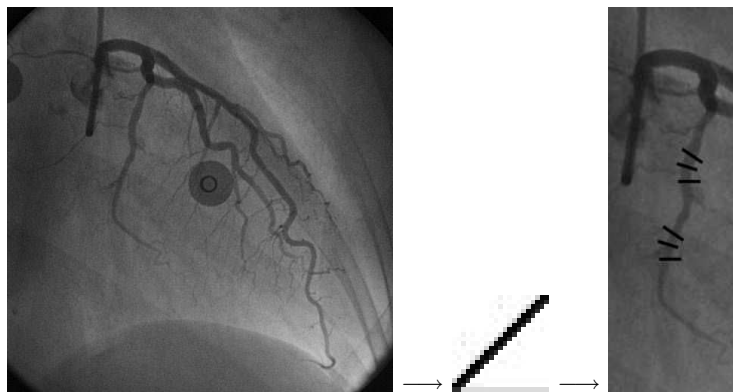


**Figure 1.** Opening an angiography image by a line-segment in one direction leads to elimination of vessels' sections in the orthogonal direction

Therefore the original image is opened by a *linear* SE with different orientations, leading thus to background images rid of vessels in the orthogonal direction. Background images are subtracted from the original one and the resulting image is built out of the maximum of all difference values at each pixel. The linear Tophat operator is given by:

$$TH_{lin}(f) = \bigvee_{i=0}^{180} TH_{\gamma_i}(f) = \bigvee_{i=0}^{180} f - \gamma_i(f),$$

where  $i$  denotes the orientation used for the linear SE.

## 2.2. Modified Gabor Filter (MGF)

The observation of gray-level profile of an X-ray angiography induces the usage of Gaussian to extract vessels (s. Figure 2). Especially small vessels can be extracted by using an angle dependent convolution mask based

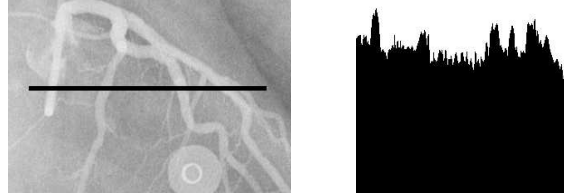


**Figure 2.** Vessels gray-level profile can be modelled by Gaussians.

on the second derivative of the Gaussian. We designed the convolution mask by combining a Gaussian-kernel in  $y$ -direction:  $k_2 e^{-\lambda y^2}$  and a kernel in  $x$ -direction:  $(1.0 - k_1 \sigma x^2) e^{-\sigma x^2}$  according to the following equation:

$$f(x, y) = k_2 e^{-\lambda y^2} (1.0 - k_1 \sigma x^2) e^{-\sigma x^2},$$

$\sigma$  and  $\lambda$  denote the standard deviations in both directions.  $k_1$  and  $k_2$  are scaling factors. The width of the Gaussian reflects the width of the vessels, we are looking for. Figure 3 illustrates the designed mask.

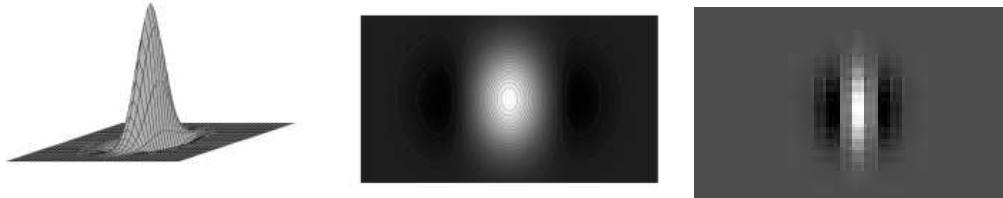


**Figure 3.** The convolution mask. From left to right: 3D view, view as a function from  $R^2$  to  $R$ , view after discretization.

Due to its *oval* form, the designed mask has the advantage to easily adapt to the curved, tubed form of vessels, as it can be seen in figure 4. The original image is filtered by the convolution mask, having various orientations, giving thus an indication not only on the existence but also on the orientation of a vessel. The result of this step is built out of the results of the different convolution masks by taking the maximum.

## 2.3. A Combined Approach to Coronary Tree Extraction

The usage of the Tophat operator is appropriate to separate the background and extract clearly visible vessels. Due to the smoothing introduced by the opening operation, vessels with small radius could get lost. Using the Gaussian masks with small width enables to recover finer vessels. A combination of both approaches increase the robustness of the extraction of the coronary-tree. We propose to combine the results of both steps by simply taking the maximum of both resulting images. It is obvious that the combination requires a gray-value scaling of the resulting images from both operations.

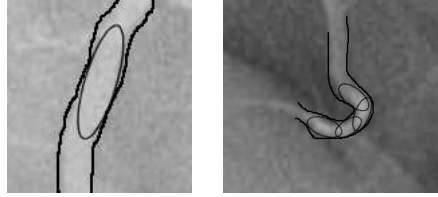


**Figure 4.** Convolution mask easily adapts to the tubed, curved vessel structure.

### 3. ANALYSIS OF CORONARY-TREE

The goal of the analysis of coronary-tree is to help the physician by *quantitative measures* to follow the recovery of vessels before and after angioplasty. To this purpose we propose to extract the centerlines of the coronary-tree, and to save the information needed for analysis in a representative graph. The nodes of the graph reflect the bifurcations of vessels, and its edges represent numerated vessel segments. Reliable information about orientation, diameter and contrast of vessels as well as the depth of branching-out and the count of visible vessels in the coronary-tree is saved in the graph. These quantitative measurements serve as indicators for categorizing the state of recovery of the patient and can be compared to earlier or later disease-stages. Section 3.1 describes shortly the method of centerline extraction. Section 3.2 discusses the extraction of bifurcations and the graph structure.

#### 3.1. Centerline Extraction

We used the method of homotopic thinning<sup>7,8</sup> to extract the centerline of vessels. This method is based on a local criterion and operates on binary images. Assuming black background the basic idea is to remove pixels on the border of white objects without changing the topology of the image. Pixels which can be removed in such a way are called *simple*. In 2D, a pixel is simple if the numbers of foreground and background connected components<sup>7</sup> remain the same after and before pixel removal. So a pixel should not be eliminated if e.g. this action splits an object component into two parts or merges two background components. On the other hand, simple pixels that constitute line extremities must be preserved. The border of the vessels will be iteratively removed, until 1-pixel lines are obtained. The number of iterations is basically given by the largest width of the vessels. We obtain thus a skeleton of the coronary tree with pixel precision. For further details on the local characterization of simple points in 2D and 3D binary images, see Bertrand and Malandain.<sup>8</sup>

#### 3.2. Extraction of Bifurcations and Crossings

The crucial step in the analysis of coronary-tree is the recognition of bifurcations and crossings in the binary skeleton, since just the bifurcations are needed to construct the nodes of the analysis graph. We adopt a morphological approach to differentiate between these structures.

We design a set of structure elements that represent the patterns that crossings and bifurcations can have in a skeleton with 1-pixel precision (1-pixel-skeleton). Crossings are located by eroding the binary image with two SEs as they are shown in figure 5. The left mask represents the crossing of two perfectly horizontal and vertical centerlines, whereas the right SE is observed when the centerlines have other directions.



**Figure 5.** Possible crossings' patterns in a 1-pixel-skeleton

Bifurcations can have three different patterns as it is listed in figure 6 (left column). Different orientations of centerlines lead to the same patterns but rotated by 90°, 180° and 270°. The obtained SEs are illustrated

in figure 6. The results of erosion with each of these SE are afterwards summarized by ‘logical and’ in a result image that will serve as a base for graph representation.

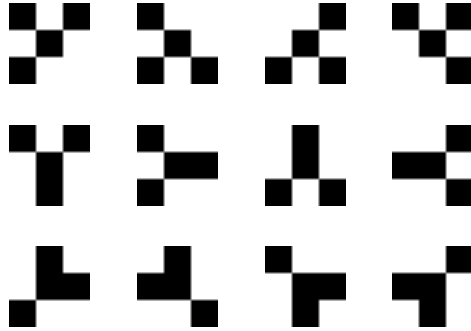


**Figure 6.** Possible bifurcations’ patterns in a 1-pixel-skeleton. From left to right: three possible bifurcations’ patterns, rotations by  $90^\circ$ ,  $180^\circ$  and  $270^\circ$ .

The graph is a binary tree having as main node the first bifurcation detected from the top of the skeleton. Each following bifurcation defines a new node in the graph. The edges of the graph are defined by the connecting vessels, which are specified by an identification number. Each node contains the following information:

- Identification number specifying the position of the current node in the graph.
- Width of the vessel from which the bifurcation emerges.
- Orientation of the centerline of the emerging vessel.
- Average gray level around the bifurcation center, which serves as an indicator for the flow of the contrast fluid.

These quantitative measurements serve as indicators for categorizing the state of recovery of the patient and can be compared to earlier or later disease-stages.

## 4. EXPERIMENTS

In order to assess the effectiveness of the approach we performed experiments using 20 X-ray angiographies, gained from a C-arm device. The angiographies are  $512 \times 512 \times 8$  bit gray-level images. We evaluated the results of the method by comparing them with the results of a hand-segmented sample of images.

### 4.1. Extraction of Coronary-Tree

Both LTO and MGF operators were applied using 8 different discrete directions. Considering the maximal vessel width, the length of the SE of the LTO was set to 21 pixel. The images were filtered by the MGF in two passes: in the first pass large vessels were extracted with  $\lambda = 20$  and  $\sigma = 8$ , and in the second smaller ones were considered:  $\lambda = 8$  and  $\sigma = 3$ . The scaling factors  $k_1$  and  $k_2$  were computed automatically for every filter mask in order to correct the gray value variance of the filter that is caused by rotation. The results of both filters are combined by taking the maximum value of the resulting images. The result is binarized by a simple threshold. Centerlines were then extracted as described in section 3.1. Figure 7 shows the resulting images at each step of the approach.

The extraction of vessels is crucial for further analysis. Errors made in this stage will remain and cause wrong analysis. The Evaluation of the *correctness* and *completeness* of the extracted coronary-tree will give a quantitative confidence measure for the method. To this purpose we compared the automatic results with hand-segmented samples, that were drawn using a graphic-board. This has been done for 10 images taken from

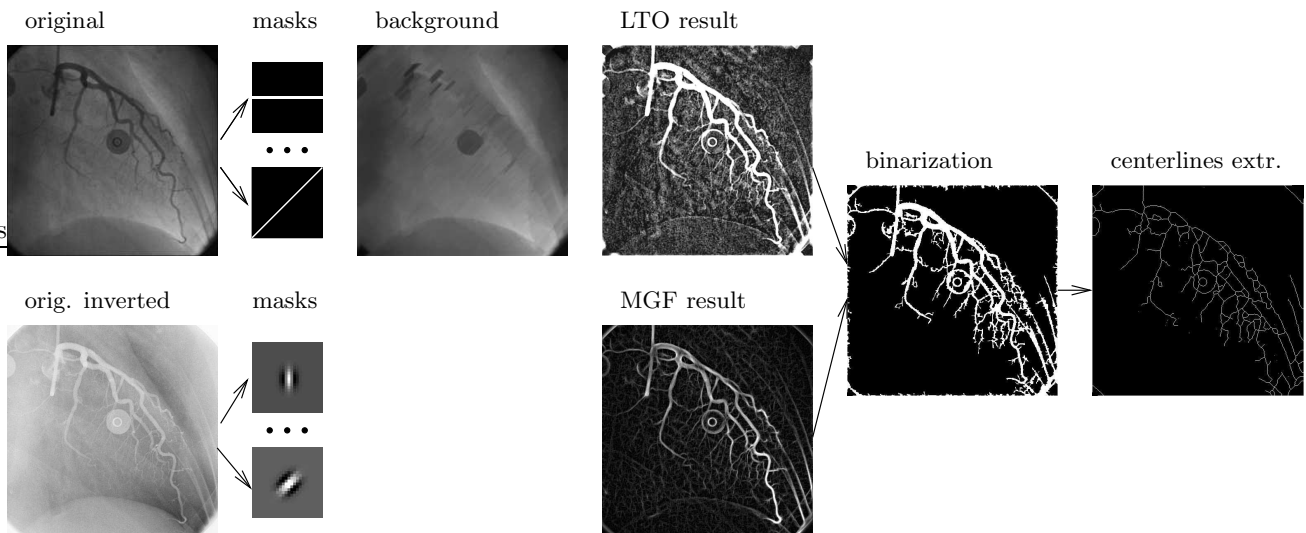


**Figure 7.** Extraction of coronary-tree

three different C-arm sequences corresponding to two different patients. The images of the first patient (img1 to img6), even taken at different times (each three are taken from a different sequence), have an ideal quality with clear shapes and few noise in the background. The angiographies of the second patient are rather noisy with barely visible vessels. Figure 14 shows the images used for evaluation. We differentiate three cases  $F_1$  to  $F_3$  while taking the hand-segmented images as reference:

- $F_1$  correct: vessels are automatically detected and they are at the same position as in the reference image. A Deviation of 2 pixels outside the reference centerline is tolerated.
- $F_2$  false-positive: vessels are automatically detected, but are not in the reference image. (more than necessary)
- $F_3$  false-negative: vessels are present in the reference image, but are not detected automatically (not found). This also includes vessels diverging from reference centerlines by more than the intended threshold.

Figure 8 visualizes the three different cases. The results of evaluation are listed in table 1.



**Figure 8.** Comparison of hand-segmented and automatically detected vessels. From left to right: hand-segmented centerline, automatically detected centerlines, superposition of both.

**Discussion:** By using the LTO it is unavoidable to recover a part of noise after subtraction due to the smoothing introduced by the opening operation. Having noisy images (img7 to img10) the effect is observable in the number of missing vessels, which are mostly small ones, having small contrast with respect to the background. In most of the images, more vessels were detected than actually present. This is partly due to the automatic detection

Images	img1	img2	img3	img4	img5	img6	img7	img8	img9	img10	Mean	Variance
# Pixels	2324	3816	4601	2129	3328	5269	3646	4935	5477	6185		
$F_1$	80.8	90.5	73.1	69.7	67.9	55.7	74.8	74.0	74.2	63.4	72.41	8.93
$F_2$	20.9	40.9	29.3	46.5	33.8	15.8	62.9	36.9	37.8	18.1	34.29	13.56
$F_3$	19.3	14.7	19.5	6.2	5.7	14.4	30.6	26.6	25.3	36.0	19.83	9.45

**Table 1.** Evaluation result of automatic coronary-tree detection. All values are given in percent with respect to the total number of pixels in the reference hand-segmented image (first row).

of the catheter, which could not be recognized as background, and is also due to image borders which were not excluded from the evaluation. Besides the centerline extraction has the tendency to connect vessels, especially at bifurcations, which leads to more skeleton pixels (s. Fig. 8, on the right). we believe that a better sub-pixel extraction method<sup>1</sup> would improve the results, by increasing the correctness rate (currently at 72.41%) and reducing both false-positive and false-negative rates.

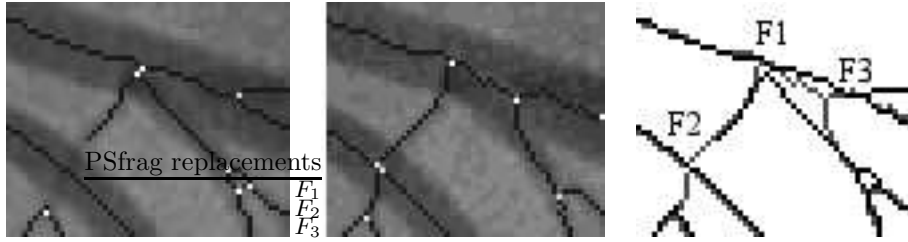
## 4.2. Analysis of Coronary-Tree

We applied the morphological erosion by the SEs designed in section 3.2 to obtain crossings of vessels as well as bifurcations. An example of a labelled image with the automatic detected structures is shown in figure 9.



**Figure 9.** A sample of automatic crossings and bifurcations detection. Left: original image. Right: original image superposed with the automatically extracted skeleton showing the results of automatic bifurcation and crossing detection.

In order to evaluate the results of this step, we proceeded in a similar way as for centerline extraction. We considered three cases of correct detection ( $B_1$ ), false-positives ( $B_2$ ) and false-negatives ( $B_3$ ). Their definition is the same as for centerline extraction. The three possible cases are illustrated in Figure 10. For  $B_1$  and  $B_3$  we tolerated a deviation of 11 pixels a part from the reference bifurcations. We evaluated the method using the same set of 10 images shown in figure 14, and taking as reference a hand-segmentation for bifurcations and crossings.



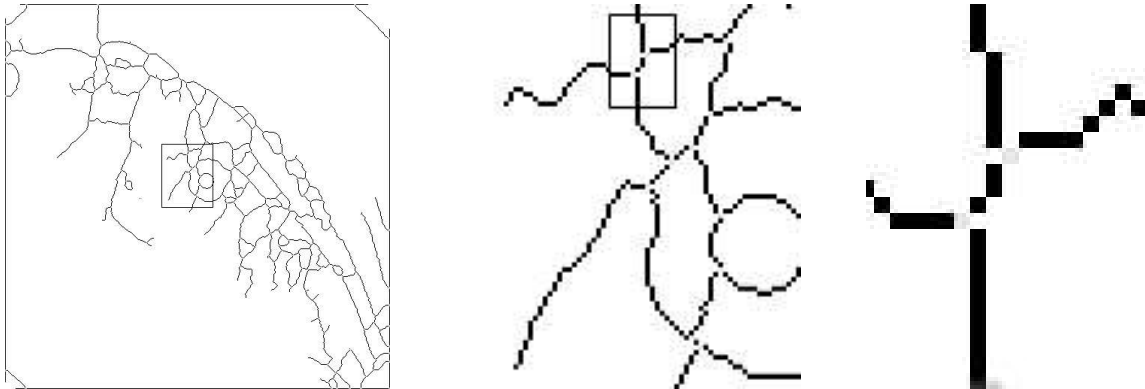
**Figure 10.** Comparison of hand-segmented and automatically detected vessels. The first image shows the the bifurcations and crossings of a hand-segmented image, the second image the result of our method. In the third image we compared the two lines by overlying them.

Table 2 summarizes the obtained evaluation results. We did not distinguish between bifurcations and crossings because crossings have mostly not been detected with the masks of section 3. Their independent evaluation would not give representative results.

images	img1	img2	img3	img4	img5	img6	img7	img8	img9	img10	Mean	Var.
# bifurcation	77	109	104	28	50	105	94	146	165	195		
$B_1$	35.0	39.4	44.2	85.7	76.0	65.6	39.3	34.8	30.9	26.6	47.75	16.81
$B_2$	37.6	65.1	68.2	217.8	248.0	81.8	116.5	49.9	58.7	30.7	97.43	58.00
$B_3$	64.9	60.5	55.7	14.2	24.0	34.2	60.5	64.9	69.0	73.2	52.11	16.78

**Table 2.** Evaluation result of the automatic detection of bifurcations and crossings. All values are given in percent with respect to the total number of bifurcations and crossings in the reference hand-segmented image (first row).

**Discussion:** As it can be observed in table 2, the correct detection rate is highly dependent on the image considered. Several factors influence negatively the detection. A first problem is related to the misclassification of crossings. In fact a crossing can be detected as two bifurcations when two vessels intersect in a segment and not in a point. Figure 11 visualizes this case.



**Figure 11.** Misclassification: A crossing is detected as two bifurcations, because the intersection area is more than one pixel. From left to right: Zooming in from original skeleton to the detected bifurcations.

A second problem is related to the amount of noise around the centerline of vessels. This noise leads to stubble in the skeleton and therefore also to far more bifurcations than existent. The effect is illustrated in figure 12.

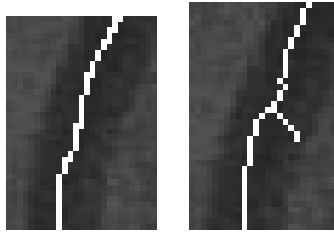


**Figure 12.** Effect of noise on detection of bifurcations and crossings: stubble in centerline extraction.

A third problem is due to the chosen skeletonisation method. In fact, a lot of bifurcations have been detected, but too far from their original position. This shifting of bifurcation point is primarily caused by the homotopic thinning, that places the bifurcation point to the barycenter, the point which has the same distance from every border. This must not always correspond to a real bifurcation (s. figure 13).

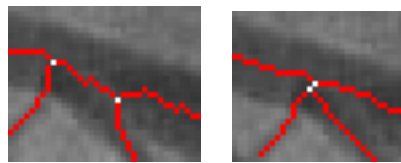


**Figure 13.** Effect of shifting of bifurcation point due to the homotopic thinning. Left: ideal detection. Right: automatic result

These problems influence the built graph, since this later deviates from binary-tree to give a directed graph instead. In order to get an representative graph of the vessel structure it would be necessary to distinguish between real vessel bifurcations and bifurcations caused by a crossing. This issue will be considered in future work.

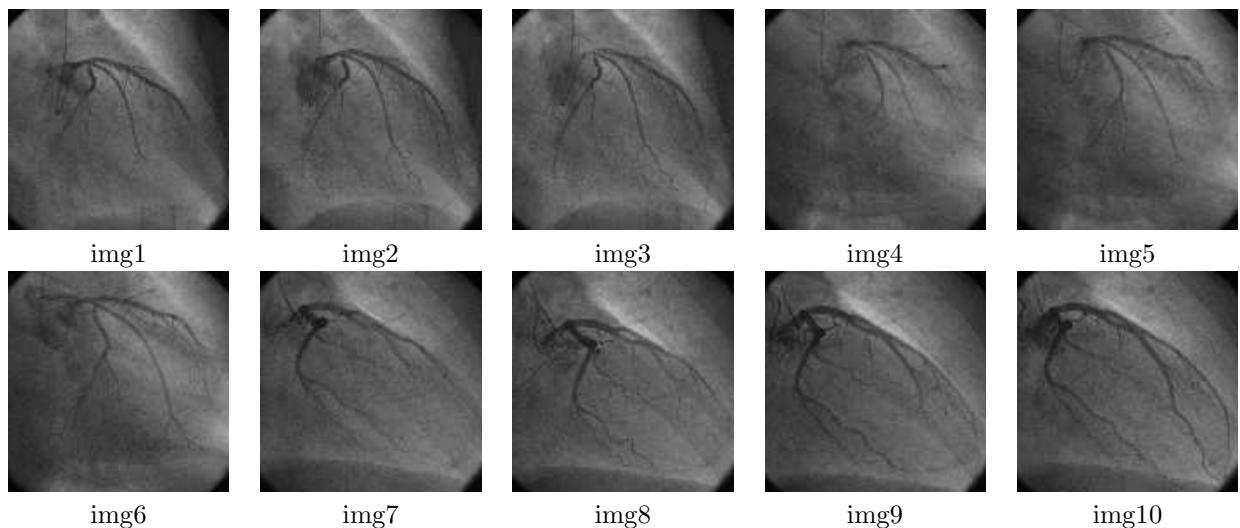


**Figure 14.** Angiographies used for evaluation: img1 to img 6 belong to the same patient. Each three were taken at different time. img7 to img120 belong to a second patient

## 5. CONCLUSION

In this article we presented an approach to segment, skeletonize and analyze coronary arteries from x-ray angiographies. A quantitative evaluation of the results of vessel extraction and bifurcation analysis allowed to objectively evaluate the correctness and completeness of the method.

Future work will concentrate on an extension of the centerline extraction step to perform sub-pixel precise location of the centerlines, and also on the improvement of the Gaussian convolution mask. We believe that this could also improve the results of the bifurcation analysis. The usage of better acquisition modalities would be also helpful.

## ACKNOWLEDGMENTS

We thank Pr. J.L. Dubois-Randé and Dr. E. Teiger (Henri Mondor Hospital, Créteil, France) for their support and for the data used in this study.

## REFERENCES

1. C. Steger, "An unbiased detector of curvilinear structures," *IEEE Transactions on Pattern Analysis and Machine Intelligence* **20**, pp. 113–125, feb 1998.
2. C. Blondel, R. Vaillant, F. Devernay, G. Malandain, and N. Ayache, "Automatic trinocular 3d reconstruction of coronary artery centerlines from rotational x-ray angiography," in *Computer Assisted Radiology and Surgery 2002 Proceedings*, Springer Publishers, Heidelberg, (Paris), jun 2002. International Symposium on Cardiovascular Imaging - Invasive Coronary and Vascular Imaging.
3. T. Lindeberg, "Scale-space: A framework for handling image structures at multiple scales," report, KTH, Kungliga Tekniska Hgskolan, S-100 44 Stockholm, Sweden, September 1996.
4. M. Hemmendorff, "Motion estimation and compensation in medical imaging," Dissertations Thesis 703, Insitute of Technology, Linkpings University, Department of Biomedical Engineering, Linkpings University, SE-581 85 Linkping, Sweden, July 2001.
5. C. Bondel, R. Vaillant, G. Malandain, and N. Ayache, "3d tomographic reconstruction of coronary arteries using a precomputed 4d motion field," tech. rep., INRIA, 2004 route des Lucioles, 06902 Sophia Antipolis, France, 2003.
6. P. Soille, *Morphological Image Analysis- principles and applications*, 2003.
7. T. Y. Kong and A. Rosenfeld, "Digital topology: introduction and survey," *Comp. Vision, Graphics and Image Proc.* **48**, pp. 357–393, 1989.
8. G. Bertrand and G. Mandalain, "A new characterization of three-dimensional simple points," *patter recognition letters* **15**, pp. 169–175, February 1994.